Two-Component Wave Equations

J. SERPE
University of Liège, Belgium
October 4, 1949

IN a recent note Jehle[1] has considered the system

$$\gamma^k(\partial_k - i\varphi_k)\psi = \mu\psi^* \tag{1}$$

involving a two-component wave function ψ and its complex conjugate ψ^*; the notation $\partial_k (k=0, 1, 2, 3)$ is used for $\partial/\partial x_k$; φ_k is a real external four-potential, μ a real constant; the four matrices γ^k and their complex conjugates γ^{k*} obey the rules

$$\tfrac{1}{2}(\gamma^{k*}\gamma^\lambda + \gamma^{\lambda *}\gamma^k) = -g^{k\lambda} I, \tag{2}$$

where I denotes the unit matrix, and

$$g^{00}=1, \quad g^{11}=g^{22}=g^{33}=-1, \quad g^{k\lambda}=0 \quad \text{if} \quad k\neq\lambda.$$

Kilmister[2] has investigated an aspect of the relationship of such two-component equations to Dirac's system.

The object of this letter is to show that Jehle's equations may be used to describe Majorana particles[3] interacting with a pseudovector field.

We first split ψ and γ^k into their real and imaginary parts, putting

$$\psi = \psi_R + i\psi_I, \tag{3}$$

$$\gamma^k = \gamma_R{}^k + i\gamma_I{}^k. \tag{4}$$

Since ψ_R and ψ_I have two components we may write the wave function as a four-row real matrix

$$\Psi = \begin{vmatrix} \psi_R \\ \psi_I \end{vmatrix}. \tag{5}$$

In this way the system (1) may be written

$$\Gamma^k(\partial_k - \Gamma\varphi_k)\Psi = \mu\Psi, \tag{6}$$

where

$$\Gamma^k = \begin{vmatrix} \gamma_R{}^k & -\gamma_I{}^k \\ -\gamma_I{}^k & -\gamma_R{}^k \end{vmatrix}, \qquad \Gamma = \begin{vmatrix} \cdot & \cdot & -1 & \cdot \\ \cdot & \cdot & \cdot & -1 \\ 1 & \cdot & \cdot & \cdot \\ \cdot & 1 & \cdot & \cdot \end{vmatrix}. \tag{7}$$

Using Eqs. (7) and (2), we find that the Γ^k obey Dirac's anticommutation relations, i.e.:

$$\tfrac{1}{2}(\Gamma^k\Gamma^\lambda + \Gamma^\lambda\Gamma^k) = -g^{k\lambda} I. \tag{8}$$

The Γ^k are real. Moreover it can be seen on the examples given by Jehle that Γ^1, Γ^2, Γ^3 and $i\Gamma^0$ may be taken as Hermitian; they give then a Majorana representation of Dirac's matrices. We also see that Γ anticommutes with the four Γ^k and that $\Gamma^2=-1$. Thus

$$\Gamma = \pm i\Gamma^5, \tag{9}$$

where

$$\Gamma^5 = i\Gamma^0\Gamma^1\Gamma^2\Gamma^3. \tag{10}$$

Both signs in Eq. (9) may occur, as can be seen directly on the two special examples given by Jehle.

Finally, Jehle's system becomes

$$\Gamma^k(\partial_k \pm i\Gamma^5\varphi_k)\Psi = \mu\Psi. \tag{11}$$

This equation, with Ψ quantized, may describe Majorana particles of "charge" ± 1 interacting with a pseudovector field φ_k. Considered from this point of view, it is covariant for the complete Lorentz group including reflections.

Jehle's formulation of Majorana's theory is easily extended to the case where there is an interaction with a real scalar field S and a real pseudoscalar field P. In this more general case, the wave equation can be written (assuming unit "charges")

$$\gamma^k(\partial_k - i\varphi_k)\psi = (\mu + S + iP)\psi^*. \tag{12}$$

[1] H. Jehle, Phys. Rev. **75**, 1609 (1949).
[2] C. W. Kilmister, Phys. Rev. **76**, 568 (1949).
[3] E. Majorana, Nuovo Cimento **14**, 171 (1937).

The Effect of Nuclear Shells upon the Pattern of the Atomic Species

WILLIAM D. HARKINS
University of Chicago, Chicago, Illinois
September 6, 1949

THE principle of regularity and continuity of atomic species, as developed by the writer, continues the thorium radioactive series down through the stable species to helium 4, and the uranium series to neon 22 and on to hydrogen 2. Harkins and Popelka[1] have shown that all of the species of the uranium series from Pb 206 to H 2 are stable, with the exception of Sr 90, which is adjacent to, but not at the end of the 50-neutron shell. In the thorium-helium series 5 are unstable, but all of these are near, but not at, the end of the 50- or 82-neutron shells.

The purpose of the present communication is to exhibit other effects of these "magic numbers" upon the pattern of the stable atomic species. It is shown that the *neutron magic numbers* have a much greater effect than the corresponding proton numbers.

Figure 1 gives the pattern in such a form as to emphasize the limits of the valley of stability, which, on account of the existence of series, are somewhat irregular. The "magic" neutron numbers are represented by lines which are somewhat curved. The lower limit of stability is of interest. Up to MN 20 it lies on the x axis $N/P=1$, or the isotopic number $I=0$. Above that no stable species lies below the straight line from ${}_{20}{}^{20}Ca_0{}^{40}$ to ${}_{80}{}^{116}Hg_{36}{}^{196}$, where the values represent ${}_P{}^N E_I{}^A$, where E is the element in question, P is the proton or atomic number, I, the isotopic number, or number of extra neutrons and A the atomic mass.

Figures 2a and 2b present the simplest plot. This gives all of the stable species. Also the naturally radioactive species of the U and Th series above ${}_{81}Tl$. The most abundant species are designated by a line around the symbol, and those below or slightly above 1 percent of the element by an open circle. Above $P=32$ these rare isotopes have the lowest neutron content, below this often the highest.

Very marked is the fact that for neutron $MN=50$ there are 6 species and 3 of these are the most abundant for the element. For neutron $MN-82$ ($MN=$magic number) there are 7 species with 5 the most abundant for the element.

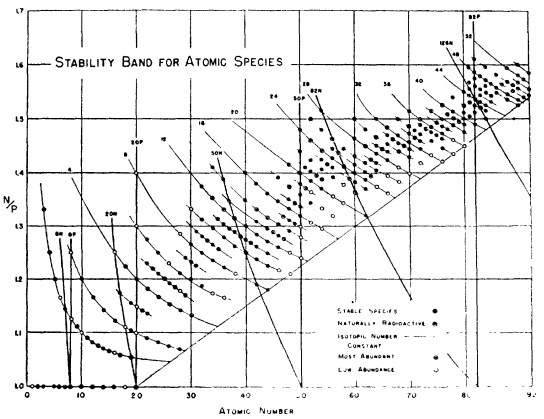

FIG. 1. Valley of stability. Heavy lines indicate ends of shells. N—neutron shell; P—proton shell.

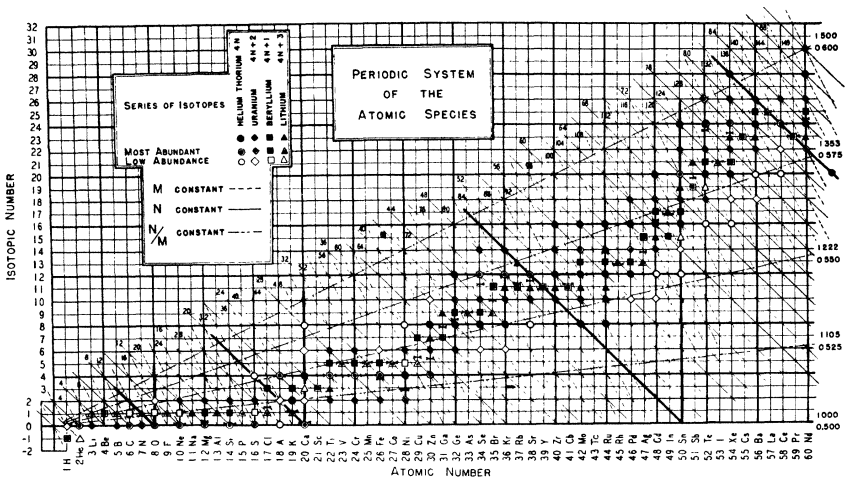

FIG. 2a. Stable atomic species to atomic number $P=60$. Heavy lines indicate ends of shells. N—neutron shell; P—proton shell.

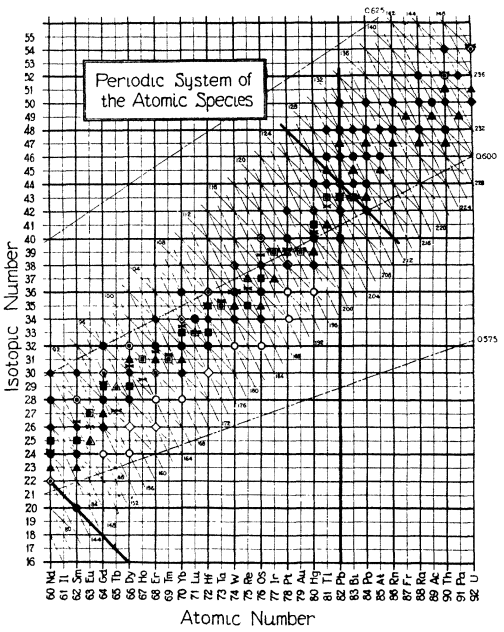

FIG. 2b. Stable atomic species. Atomic number $P=60$ to 81. Heavy lines indicate ends of shells. N—neutron shell; P—proton shell.

The most marked effect of a proton MN is shown at calcium = 20 where $_{20}{}^{28}Ca_8{}^{48}$ would presumably not exist if it were not at the end of a proton shell. This distorts the pattern. The region of few isotopes is just below this, but the neutron MN 20 gives 4 species with 2 of them the most abundant for the element. The 82-proton and 126-neutron magic numbers extend into the region of natural radioactivity, but even there the former is represented by 3 stable isotopes and the latter by 2, and both of these 2 are the most abundant isotopes.

A chart which emphasizes the effect of "magic numbers" on existence and isotopic number (extra neutrons) of the most abundant isotope is presented in Fig. 3, where the values for the *odd* elements are connected by a line, and those for the even elements are not so connected. It is remarkable that for $P=9$ to 30 the number of extra neutrons (I) is represented by higher values for odd than for even elements, but for 32 to 77 the values of I for even elements lie above the line for odd elements. The shift occurs just where the region of abundant species changes to that of rare species. Just at Ni_{28}, where the shift occurs, the number of extra neutrons becomes specially low (2).

The remarkable feature of the figure is the break which occurs just above the 50- and the 82-*neutron shells*. Here element 43, *which has no stable isotope*, lies just above the end of the 50-neutron shell, and 61, again with no stable isotope, just above the end of the 82-neutron shell. Neither the proton shells nor the 20- or 126-neutron shells have such a marked effect upon the relations discussed here.

In a paper submitted in July the abundance of nuclear species is considered in terms of even and odd P and even and odd N. This shows in a much more marked way the effects of the proton "magic numbers." This method of treatment of even and odd P was introduced in 1915 (1920 for even and odd N) by the writer, but even yet prominent workers classify according to even or odd $A=P+N$, which obscures certain of the relations, since odd +odd = even.

The effect of a proton magic number may be illustrated by tin at the ends of the 50-proton shell. Since the number of protons is greater than 30 it is a somewhat rare element. However, the effect of the end of the shell is shown by the fact that *it is much more abundant than any other element from $P=41$ to $P=92$*, and is, for example, 24 times more abundant than cadmium ($P=48$), which has the next lower even atomic number.

In 1915–17 the writer developed what has become known as Harkins rule, that the elements of even number are very much more abundant than those of odd number. However, the remainder of the rule is usually forgotten. This is that the atomic species which contain an even number of neutrons are very much more abundant than those in which the number is odd.

Thus 2 is the most important of the magic numbers. This is

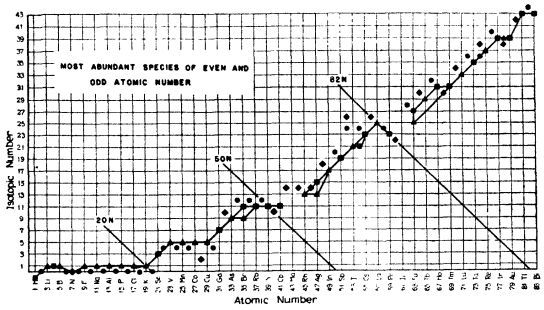

FIG. 3. Most abundant isotopes of the elements of odd and of even atomic number. Heavy lines indicate ends of shells. N—neutron shell; P—proton shell.

illustrated by helium p_2n_2 *whose cosmic abundance, according to the latest estimate, is 120 times greater than that of* **all** *of the other elements*, excluding hydrogen, which has a simple nucleus. This shell of 2 neutrons or of 2 protons has not received the attention which it merits.

For a discussion of closed shells with 20, 50, 82 neutrons or protons, or 126 neutrons, a paper by Maria Mayer may be consulted.[2]

[1] W. D. Harkins and M. Popelka, Jr., Phys. Rev. **76**, 989 (1949).
[2] M. G. Mayer, Phys. Rev. **74**, 235 (1948).

The Ratio of L_I to K Capture*

M. E. Rose and J. L. Jackson**
Oak Ridge National Laboratory, Oak Ridge, Tennessee
September 29, 1949

THE phenomenon of orbital electron capture from the L_I shell was observed recently by Pontecorvo, Kirkwood, and Hanna[1] in A^{37}. The experimental value of the ratio of probabilities for L_I to K capture was reported to be between 8 and 9 percent. As was mentioned in reference 1 a computed ratio of only 6 percent is obtained using relativistic wave functions with Slater screening constants.[2]

It is possible to use a much better representation of the screening and we have calculated the L_I to K capture ratio using (1) relativistic wave functions computed on the Eniac by J. Reitz[3] with a potential function obtained from a Thomas-Fermi field with exchange and (2) self-consistent field wave functions.[4] In the case of the relativistic wave functions the small screening for the $1s$ wave function was not considered and an extrapolation had to be carried out since the $2s$ wave functions are available for $Z=29$, 49, 84 and 92 only. Since the ratio is not very sensitive with Z (see Fig. 1), this extrapolation seems safe enough. The Hartree wave functions used for A included the effect of exchange and the neglect of non-relativistic effects makes a rather trivial error in the case of A. The results are:

	L/K ratio
(1) relativistic wave functions	8.2 percent
(2) Hartree wave functions	8.1 percent

and the agreement with the observed value is all that could be desired.

The L/K ratio for other values of Z may be obtained from Fig. 1, curve (1) for medium and heavy atoms and curve (2) for light atoms. In Fig. 1 the square of the ratio of the $2s$ to $1s$ wave functions at the nuclear radius is shown. The L/K capture ratio is obtained by multiplying by the square of the ratio of neutrino energies in the two cases,[2] but in almost every case this latter ratio should be very close to unity.

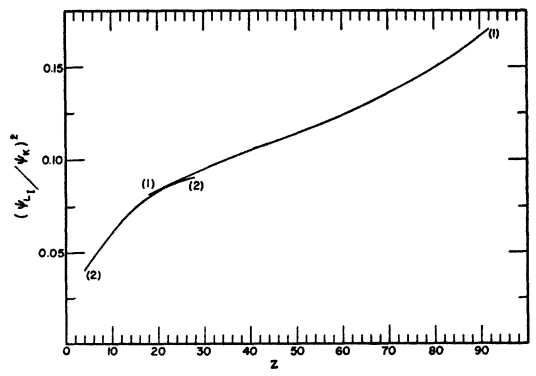

FIG. 1. Ratio of electron densities for L_I and K shell at nuclear radius *versus* Z: Curve (1): relativistic wave functions with Thomas-Fermi field plus exchange. Curve (2): Hartree self-consistent field wave functions. To obtain ratio of L_I to K capture multiply by square of ratio of neutrino energies in the two cases, $(E_{L_I}/E_K)^2$.

* This document is based on work performed under Contract No. W-7405, eng 26 for the AEC at the Oak Ridge National Laboratory.
** Present address, New York University.
[1] Pontecorvo, Kirkwood, and Hanna, Phys. Rev. **75**, 982 (1949).
[2] R. E. Marshak, Phys. Rev. **61**, 431 (1942).
[3] The authors are indebted to Dr. Reitz for a pre-publication copy of these wave function tables.
[4] Complete references are to be found in D. R. Hartree, Reports on Progress in Physics, XI (1946–47).

The Disintegration Scheme of Tm^{170}

J. S. Fraser
Radiation Laboratory, McGill University, Montreal, Quebec, Canada
September 27, 1949

NEW evidence for the complexity of the beta-ray spectrum of 127-day Tm^{170} has been obtained by the use of a thin lens spectrometer supplemented by β-γ-coincidence measurements. The beta-ray spectrum has been shown to consist of two components; one with a maximum energy of (970±5) kev as reported previously, and a second with an endpoint of (886±5) kev comprising approximately 10 percent of the transitions. The single weak gamma-ray,[1-4] largely internally converted, has been found to have an energy of (83.9±0.2) kev.

The source was prepared from "Specpure" Tm_2O_3 irradiated in the Chalk River pile to give a specific activity of 5 mc/mg. The source thickness was estimated to be 0.25 mg/cm² and it was mounted on a 0.03 mg/cm² Nylon film rendered conducting by a layer of evaporated aluminum (0.02 mg/cm²). The counter window was made up of Nylon films to a thickness of 0.055 mg/cm² and passed electrons of energy greater than 7 kev. Good statistics were obtained and the high energy end of the spectrum was studied carefully. The Kurie plot of the beta-spectrum using the relativistic coulomb correction factor is shown in Fig. 1. If the assumption is made that the higher energy group is of the allowed shape, then the discontinuity in the Kurie plot is indicative of a weak beta-ray group of lower maximum energy. Subtraction of the main group from the total yields a reasonably straight line which when extrapolated to the energy axis gives an end point of (900±20) kev (curve C, Fig. 1). The rise of the curve

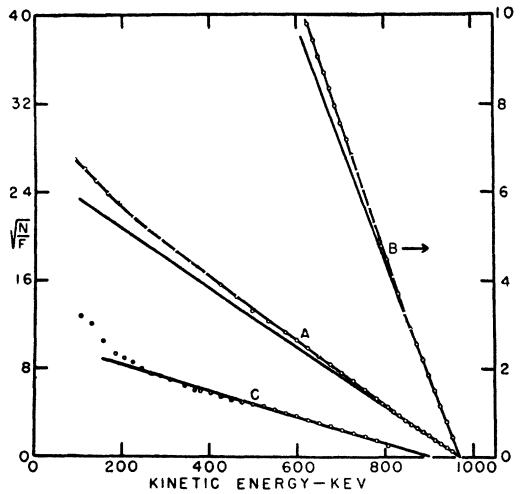

FIG. 1. Kurie plot of the Tm^{170} beta-spectrum. Curve A is the curve of the experimental points, curve B is the high energy end plotted with an expanded ordinate scale, and curve C is obtained by subtracting the main group.